Journal of Materials Processing Technology 216 (2015) 369–374

Contents lists available at ScienceDirect

Journal of Materials Processing Technology

journal homepage: www.elsevier.com/locate/jmatprotec

Mitigation of pores generation at overlapping zone during laser cladding

Chunyang Zhou, Shusen Zhao, Yibo Wang, Falan Liu, Wenyan Gao, Xuechun Lin*

Institute of Semiconductors, Chinese Academy of Sciences, Beijing 100083, PR China

ARTICLE INFO

Article history:
Received 13 February 2014
Received in revised form 18 July 2014
Accepted 30 September 2014
Available online 7 October 2014

Keywords:
Laser cladding
Pore
Generation mechanism
Controlling method

ABSTRACT

In the process of laser cladding, pores existing frequently at the bottom of overlapping zone. The generation mechanism and controlling methods of the pores are investigated. The results showed that the laser power density suddenly decreases at the bottom of overlapping zone because of the tangential angle of the cladding outline, and the lower power density slowed down the generation of the molten pool. On the other hand, the molten pool around the border position formed quickly and fused together. Then the pores formed due to the rapid solidification of the molten pool. The main factor that affects the generation of pores is the width-to-height ratio of single track because it affected the power density by the angle indirectly. Besides, a higher power density and lower thermal conductivity can restrain the generation of the pores by increasing convection intensity and convection time of the molten pool. In addition, reducing the high-melting-point hard phase may lead to smaller pores.

1. Introduction

Laser cladding is an advanced surface modification technology with a quickly melting and solidification process. Laser with a high power density is applied to melt the powder materials and limited substrate to form a cladding with metallurgical bonding. With some special powders laser cladding can improve wear resistance and corrosion resistance. For example, cladding reinforced by TiC particles revealed higher wear resistance than that of the substrate (Wang et al., 2008), and Inconel 617 provided very good corrosion protection (Mahmood et al., 2012).

Because of inappropriate processing parameters used in laser cladding and other unavoidable factors, many defects appeared in the cladding, such as pores and cracks. The generation mechanism of the defects are of significance for improving laser cladding process, therefore, a great number of studies about pores and cracks inside the cladding have been carried out. Pores may be caused by the entrapment of gas released from the fine powders (Xue and Wang, 2005), the unmelted powder injected into molten pool (Yang et al., 2002), and exothermic reactions in overheated molten pool (Buza et al., 2008). Gas trapping due to large fluid viscosity induced by WC particles in the molten pool also caused the generation of pores (Amado et al., 2009). Another reason for pore generation is that the free carbon in the powder easily combines with oxygen in the air formed CO or CO_2 (Sun et al., 2001). A small amount (1 wt.%) of aluminium powder added to the powders contained carbide can restrains the generation of pores because aluminium has a much higher affinity for oxygen (Huang et al., 2003). A model of calculating the evolution of temperature and thermal stress using different scanning patterns was proposed and the results show that the stresses, which caused cracks, are decreased with fractal scanning pattern (Ma and Bin, 2007). Otherwise, preheating can restrain the cracks effectively (Jendrzejewski et al., 2004).

Especially, some pores formed frequently at the bottom of overlapping zone during multi-track laser cladding, which has been rarely investigated. A model of multi-track laser cladding was proposed to study the pores at overlapping zone and pointed out that pores appeared when the width-to-height ratio of the single track is less than 4 (Aiyiti et al., 2006). However, the study only provided a qualitative description and no study on the mechanism of the pores was reported.

In this paper, the generation mechanism of the pores is studied both theoretically and experimentally. Also, some controlling methods for pores generation are also presented.

2. Experiment details

Low carbon steel Q235 and stainless steel 304 with the same dimension of 200 mm × 100 mm × 10 mm were used as substrate.

* Corresponding author at: Room 422, Building 1, No. A35, QingHua East Road, Haidian District, Beijing, PR China. Tel.: +86 010 82304165.
E-mail address: xclin@semi.ac.cn (X. Lin).

http://dx.doi.org/10.1016/j.jmatprotec.2014.09.025
0924-0136/

Table 1
Chemical components of substrates and powder (wt.%).

	C	Mn	Si	S	P	Ni	Cr	B	Mo	Fe
Q235	0.2	1.4	0.35	0.045	0.045	–	–	–		Bal.
SS304	<0.07	<2	<1	<0.03	<0.035	8–11	17–19	–	–	Bal.
Fe901	0.5	–	1.2	–	–	–	13	1.6	0.8	Bal.
Cr_3C_2	12–14						84–87			

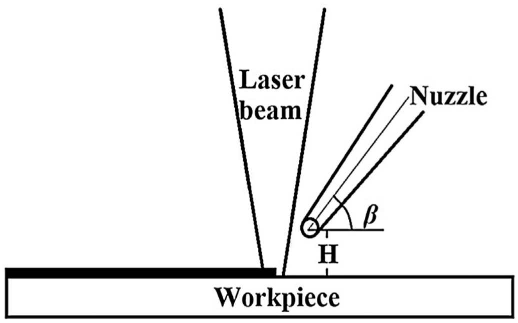

Fig. 1. Position of nuzzle.

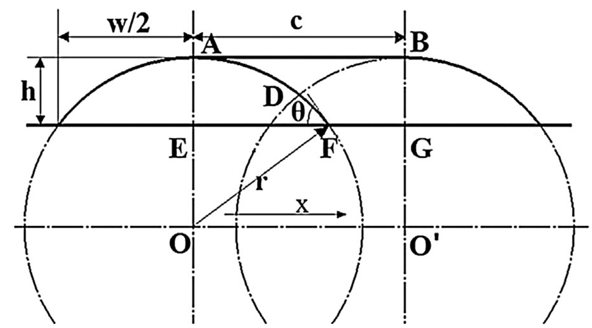

Fig. 2. Model of overlapping.

Self-fluxing alloy powder Fe901 and Cr_3C_2 were selected as the cladding materials. The size of the powder is −140 to +325 mesh. The chemical compositions of laser cladding materials are shown in Table 1. A 3000 W CW solid state laser at 1064 nm and an ABB-2400 robot were used for laser cladding process. The powder was fed synchronously and laterally, as shown in Fig. 1, and the Nitrogen was used as carrier gas, and the purity of the nitrogen is 99.999%.

The processing parameters are shown in Table 2. In the process, the flow rate of carrier gas was 3 L/min, the diameter of the powder nozzle was 2 mm, the distance of powder nozzle from substrate H was 10 mm, and the angle of the powder nozzle β was 45°.

Finally, the samples were cut in a direction perpendicular to the scanning direction of the laser beam. The samples were grinded and polished with polishing machine and the cladding is observed with an optical microscope.

3. Theoretical analysis

A model of overlapping is established to calculate the distribution of laser power density, as shown in Fig. 2. The following assumptions have been made in order to simplify the calculation:

a) The laser beam has an ideal Gaussian intensity profile and at normal incidence.
b) Direction from O to O′ is the positive direction of x.
c) The change of power density along z direction is ignored.

Power density distribution of laser beam in section ADFG showed in Fig. 2 is given by

$$q(x) = \omega(x) \cdot \cos\theta \tag{1}$$

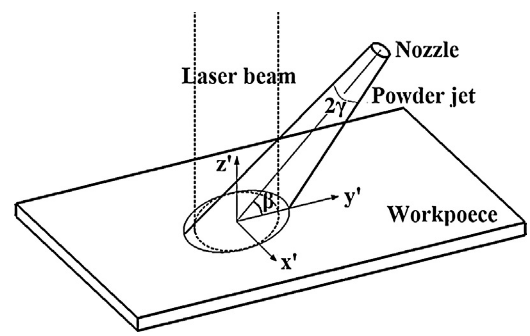

Fig. 3. Model of light and powder.

where

$$\cos\theta = \frac{\sqrt{r^2 - x^2}}{r} \tag{2}$$

$$r = \frac{h}{2} + \frac{w^2}{8h} \tag{3}$$

$\omega(x)$ is the power density distribution taking into account the influence of the powder flow, c is the scan spacing, h is the height of cladding, w is the width of cladding, r is the radius of cladding cross-section outline, θ is the tangential angle of the cladding outline.

A model of interaction of the laser beam with the powder particles was established for lateral powder feeding (Fu et al., 2002), as shown in Fig. 3. The powder jet exits from the nozzle and spread out with angle γ. We take a cylinder perpendicular to plane (x', y')

Table 2
Processing parameters.

No.	Power (W)	Size of laser sport (mm)	Velocity (mm/s)	Defocus distance (mm)	Powder flow rate (g/min)	Powder	Substrate
1	1200	5.4	5	−20	7.3	Fe901 + Cr_3C_2	Q235
2	1200	5.4	5	−20	8.5	Fe901 + Cr_3C_2	Q235
3	1200	3.7	5	−12	5.7	Fe901 + Cr_3C_2	Q235
4	1200	3.7	5	−12	6.6	Fe901 + Cr_3C_2	Q235
5	1200	5.4	5	−20	7.3	Fe901 + Cr_3C_2	SS304
6	1200	5.4	5	−20	8.5	Fe901 + Cr_3C_2	SS304
7	1200	5.4	5	−20	7.3	Fe901	Q235
8	1200	5.4	5	−20	8.5	Fe901	Q235